Neutral atmospheric influences of the solar proton events in October–November 2003

Charles H. Jackman,[1] Matthew T. DeLand,[2] Gordon J. Labow,[1,2] Eric L. Fleming,[1,2] Debra K. Weisenstein,[3] Malcolm K. W. Ko,[4] Miriam Sinnhuber,[5] and James M. Russell[6]

Received 5 November 2004; revised 6 January 2005; accepted 17 January 2005; published 14 July 2005.

[1] The large solar storms in October–November 2003 caused solar proton events (SPEs) at the Earth and impacted the middle atmospheric polar cap regions. Although occurring near the end of the maximum of solar cycle 23, the fourth largest period of SPEs measured in the past 40 years happened 28–31 October 2003. The highly energetic protons associated with the SPEs produced ionizations, excitations, dissociations, and dissociative ionizations of the background constituents, which led to the production of odd hydrogen (HO_x) and odd nitrogen (NO_y). NO_x ($NO + NO_2$) was observed by the UARS HALOE instrument to increase over 20 ppbv throughout the Southern Hemisphere polar lower mesosphere. The NOAA 16 SBUV/2 instrument measured a short-term ozone depletion of 40% in the Southern Hemisphere polar lower mesosphere, probably a result of the HO_x increases. SBUV/2 observations showed ozone depletions of 5–8% in the southern polar upper stratosphere lasting days beyond the events, most likely a result of the NO_y enhancements. Longer-term Northern Hemisphere polar total ozone decreases of >0.5% were predicted to last for over 8 months past the events with the Goddard Space Flight Center two-dimensional model. Although the production of NO_y constituents is the same in both hemispheres, the NO_y constituents have a much larger impact in the northern than the southern polar latitudes because of the seasonal differences between the two hemispheres. These observations and model computations illustrate the substantial impact of solar protons on the polar neutral middle atmosphere.

Citation: Jackman, C. H., M. T. DeLand, G. J. Labow, E. L. Fleming, D. K. Weisenstein, M. K. W. Ko, M. Sinnhuber, and J. M. Russell (2005), Neutral atmospheric influences of the solar proton events in October–November 2003, *J. Geophys. Res.*, *110*, A09S27, doi:10.1029/2004JA010888.

1. Introduction

[2] Large-scale solar explosions can result in huge fluxes of high-energy solar protons at the Earth, especially near solar maximum. A period of time wherein the solar proton flux at the Earth is elevated for a few days is known as a solar proton event (SPE).

[3] Solar protons impact both the northern and southern polar cap regions (>60° geomagnetic latitude) as a result of the charged particles being guided by the Earth's magnetic field. These protons have energies sufficient to impact the neutral middle atmosphere (stratosphere and mesosphere) and produce ionizations, dissociations, dissociative ionizations, and excitations. These atmospheric interactions result in the production of both HO_x (H, OH, HO_2) and NO_y (N, NO, NO_2, NO_3, N_2O_5, HNO_3, HO_2NO_2, HONO, $ClONO_2$, $ClNO_2$, $BrONO_2$) constituents either directly or through a photochemical sequence [e.g., *Swider and Keneshea*, 1973; *Crutzen et al.*, 1975; *Jackman et al.*, 1980; *Solomon et al.*, 1981; *McPeters*, 1986; *Zadorozhny et al.*, 1992]. These HO_x and NO_y enhancements subsequently cause decreases in ozone [e.g., *Weeks et al.*, 1972; *Heath et al.*, 1977; *Solomon et al.*, 1983; *Jackman et al.*, 1990; *Krivolutsky et al.*, 2003; *Jackman and McPeters*, 2004].

[4] A very active solar period near the end of solar cycle 23 maximum happened in October–November 2003. Several solar explosions resulted in SPEs in late October and early November 2003. An especially vigorous period of high fluxes of energetic protons occurred 28–31 October 2003. *Seppälä et al.* [2004] have shown significant effects from the October–November 2003 SPEs in the Northern Hemisphere polar winter with GOMOS/Envisat data. We provide further evidence of a large middle atmospheric impact from these SPEs using NOAA 16 SBUV/2 and UARS HALOE measurements of the Southern Hemisphere polar atmosphere. We also show global model simulations to aid in the analysis of these polar impacts.

[5] In this paper we discuss the measured and modeled impacts of the protons ejected by the Sun in October–November 2003 on the Earth's middle atmosphere. This

[1]NASA Goddard Space Flight Center, Greenbelt, Maryland, USA.
[2]Science Systems and Applications, Inc., Lanham, Maryland, USA.
[3]Atmospheric and Environmental Research, Inc., Lexington, Massachusetts, USA.
[4]NASA Langley Research Center, Hampton, Virginia, USA.
[5]University of Bremen, Germany.
[6]Hampton University, Hampton, Virginia, USA.

0148-0227/05/2004JA010888$09.00

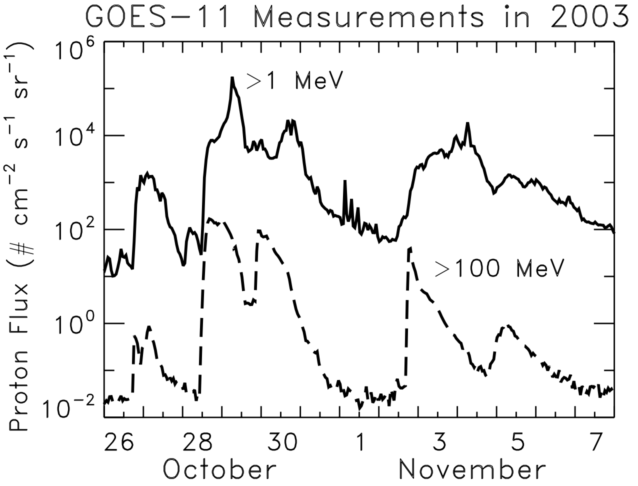

Figure 1. GOES 11 proton flux measurements in 2003 for energies >1 MeV (solid line) and >100 MeV (dashed line). These data are provided by the NOAA SEC at their Web site (http://sec.noaa.gov/Data/goes.html).

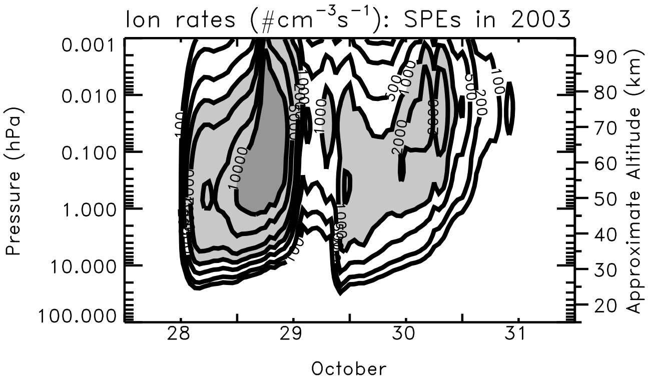

Figure 3. Ion pair production rates for 2003 using the GOES 11 proton flux measurements for 28–31 October with contour levels 100, 200, 500, 1000, 2000, 5000, and 10,000 cm^{-3} s^{-1}. The dark gray highlighted areas indicate ion production rates greater than 10,000 cm^{-3} s^{-1}. The light gray highlighted areas indicate ion production rates greater than 1000 but less than 10,000 cm^{-3} s^{-1}.

paper contains six primary sections, including the introduction. The solar proton flux measurements and energy deposition are presented in section 2. The production of odd hydrogen (HO_x) and odd nitrogen (NO_y) by the solar protons is discussed in section 3. Observations of NO_x ($NO + NO_2$) and ozone change as a result of the October–November 2003 SPEs are given in section 4. The GSFC two-dimensional model used to simulate the impact of the disturbed time period and model predictions of the SPEs' influence are presented in section 5. Finally, conclusions are given in section 6.

2. Proton Measurements/Energy Deposition

2.1. Solar Proton Flux Measurements

[6] An accessible and useful proton flux data set is provided by the National Oceanic and Atmospheric Administration (NOAA) Space Environment Center (SEC) for the NOAA Geostationary Operational Environmental Satellites (GOES) (see http://sec.noaa.gov/Data/goes.html). Proton fluxes are provided at this site in several energy intervals (>1 MeV, >5 MeV, >10 MeV, >30 MeV, >50 MeV, and >100 MeV), updated every 5 min. The GOES 11 data are considered most reliable for proton fluxes depositing energy into polar latitudes and were used as the proton flux source for this study. These proton flux measurements are given in Figure 1 for the 26 October through 7 November 2003 time period. The largest proton fluxes of year 2003 were recorded 28–30 October. Protons with energies >100 MeV are fast-moving and arrive in the near Earth environment early in the solar event. These high-energy protons deposit the bulk of their energy in the polar stratosphere. Lower-energy (and slower moving) protons with energies near 1 MeV arrive later, but fluxes at these lower energies can remain elevated for a longer period of time. These lower energy protons, between about 1 and 30 MeV, deposit the bulk of their energy in the mesosphere.

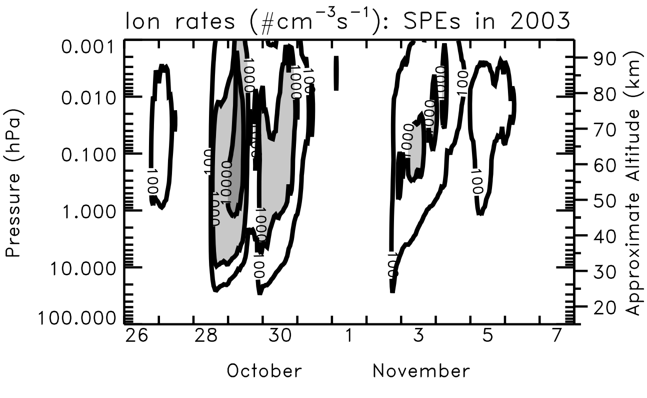

Figure 2. Ion pair production rates for 2003 using the GOES 11 proton flux measurements for 26 October through 7 November with contour levels 100, 1000, and 10,000 cm^{-3} s^{-1}. The dark gray highlighted areas indicate ion production rates greater than 10,000 cm^{-3} s^{-1}. The light gray highlighted areas indicate ion production rates greater than 1000 but less than 10,000 cm^{-3} s^{-1}.

2.2. Energy Deposition

[7] The calculation of the energy deposition of the protons in the atmosphere used a methodology discussed by *Vitt and Jackman* [1996]. Precipitating protons primarily lose their energy in the creation of ion pairs in the atmosphere. An ion pair is created when a precipitating proton removes an electron (called a secondary electron) from the neutral molecule or atom, leaving behind a positive ion. The protons impart energy onto the secondary electrons and these freed charged particles also cause further ionizations in the atmosphere.

[8] The hourly average ion pair production profiles were computed from the GOES 11 proton fluxes and are presented in Figures 2 and 3. Figure 2 shows the ion pair production rates over the entire 26 October through 7 November 2003 time period, whereas Figure 3 is an enlargement of the very intense period, 28–31 October 2003. Ion pair production rates of greater than 1000 cm^{-3}s^{-1} were computed down to 10 hPa (~32 km)

Table 1. HO_x Constituents Produced Per Ion Pair as a Function of Altitude for Baseline Ionization Rates (BIR) of 10^2, 10^3, and 10^4 $cm^{-3}s^{-1}$

Altitude, km	HO_x Production per Ion Pair[a]		
	BIR – 10^2 $cm^{-3}s^{-1}$	BIR – 10^3 $cm^{-3}s^{-1}$	BIR – 10^4 $cm^{-3}s^{-1}$
40	2.00	2.00	1.99
45	2.00	1.99	1.99
50	1.99	1.99	1.98
55	1.99	1.98	1.97
60	1.98	1.97	1.94
65	1.98	1.94	1.87
70	1.94	1.87	1.77
75	1.84	1.73	1.60
80	1.40	1.20	0.95
85	0.15	0.10	0.00
90	0.00	0.00	0.00

[a]These HO_x production rates were taken from *Solomon et al.* [1981].

during this very intense period. Very large ion rates (>10,000 $cm^{-3}s^{-1}$) were computed on 2 days, 28–29 October, throughout the polar cap in the mesosphere. Such large impacts to the polar middle atmosphere are very uncommon, typically only occurring a few times during a particular solar maximum period.

3. Odd Hydrogen (HO_x) and Odd Nitrogen (NO_y) Production

3.1. Odd Hydrogen (HO_x) Production

[9] Along with the ion pairs, the protons and their associated secondary electrons also produce odd hydrogen (HO_x) and odd nitrogen (NO_y). The production of HO_x relies on complicated ion chemistry that takes place after the initial formation of ion pairs [*Swider and Keneshea*, 1973; *Frederick*, 1976; *Solomon et al.*, 1981]. *Solomon et al.* [1981] computed HO_x production rates as a function of altitude and ion pair production. Some of these computations are given in Table 1 for background ion pair production rates of 10^2, 10^3, and 10^4 $cm^{-3}s^{-1}$. Each ion pair typically results in the production of around two HO_x constituents in the upper stratosphere and lower mesosphere (see Table 1). In the middle and upper mesosphere, an ion pair is computed to produce less than two HO_x constituents per ion pair.

3.2. Odd Nitrogen (NO_y) Production

[10] Odd nitrogen is produced when the energetic charged particles collide with and dissociate N_2. Following *Porter et al.* [1976] we assume that 1.25 N atoms are produced per ion pair. The *Porter et al.* [1976] study also further divided the proton impact of N atom production between ground state (~45% or ~0.55 per ion pair) and excited state (~55% or ~0.7 per ion pair) nitrogen atoms. Ground state [$N(^4S)$] nitrogen atoms can create other NO_y constituents, such as NO, through

$$N(^4S) + O_2 \rightarrow NO + O \tag{1}$$

or can lead to NO_y destruction through

$$N(^4S) + NO \rightarrow N_2 + O. \tag{2}$$

Generally, excited states of atomic nitrogen, such as $N(^2D)$, result in the production of NO through [e.g., *Rusch et al.*, 1981; *Rees*, 1989]

$$N(^2D) + O_2 \rightarrow NO + O \tag{3}$$

and do not cause significant destruction of NO_y. *Rusch et al.* [1981] showed that there are huge differences in the final results of model computations of NO_y enhancements from SPEs that depend strongly on the branching ratios of the N atoms produced. We currently do not include any of the excited states of atomic nitrogen (e.g., $N(^2D)$, $N(^2P)$, and N^+) as computed constituents in our model. In order to best represent the production of NO_y constituents by the protons and their associated secondary electrons, we assume that 45% of the N atoms produced per ion pair result in the production of $N(^4S)$ {~0.55 per ion pair} and that 55% of the N atoms produced per ion pair result in the production of NO {~0.7 per ion pair}.

[11] The SPEs of 28–31 October 2003 were very large and can be compared with other huge SPEs in the past. These 28–31 October 2003 SPEs were computed to have produced 3.4×10^{33} NO_y molecules. Only three other SPEs in the past 40 years were larger including the events of 19–27 October 1989 (6.7×10^{33} NO_y molecules), 2–10 August 1972 (3.6×10^{33} NO_y molecules), and 14–16 July 2000 (3.5×10^{33} NO_y molecules) [e.g., see *Jackman et al.*, 2001]. The number reported here for the July 2000 SPE is slightly larger than that reported by *Jackman et al.* [2001] since GOES 8 proton fluxes are used in this work, whereas GOES 10 proton fluxes were used by *Jackman et al.* [2001]. The GOES 8 data are considered more reliable than the GOES 10 data for proton fluxes depositing their energy in polar latitudes (T. Onsager, NOAA SEC, private communication, 2003).

4. Observations of Southern Hemisphere Polar Atmospheric Influence

4.1. Ozone

[12] The large ionization rates (see Figures 2 and 3) translate into very significant production of HO_x and NO_y. Both of these families are capable of catalytically destroying ozone. The NOAA 16 SBUV/2 satellite provides daily ozone data at particular altitudes [*Hilsenrath et al.*, 1995]. These SBUV/2 data can be turned into daily maps using interpolation along the orbital tracks and filling between successive orbits with the Delauney triangulation method discussed by *Stolarski et al.* [1997]. The six plots in Figure 4 indicate ozone amounts at 0.5 hPa (~55 km) from 27 October through 1 November 2003. The 27 October data show ozone before the most intense period of proton fluxes. Proton fluxes start to pick up on 28 October and reach peak levels on 29 October (see Figure 1). Ozone levels are reduced very significantly (20–40%) on this day. The outline of the polar cap (>60°S geomagnetic), where the solar protons are predicted to interact with the atmosphere, is indicated by the thick white oval in all plots. Other days (30 October through 1 November) show varying ozone amounts that are directly linked to the proton flux variations. Figure 4 illustrates the dramatic reduction in the ozone amounts at this level in or near the polar cap during

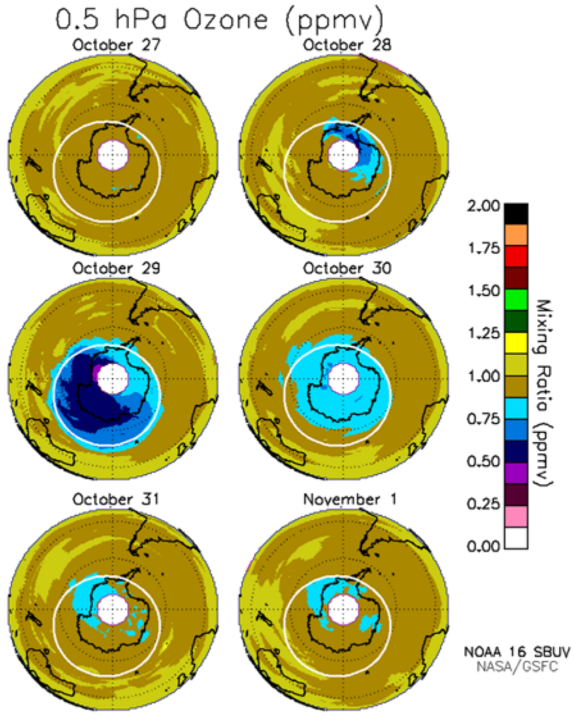

Figure 4. NOAA 16 SBUV/2 Southern Hemisphere polar ozone in ppmv for 6 days (27 October through 1 November) around the peak proton flux intensity in October–November 2003. The solid white circle indicates the southern polar cap boundary (60°S geomagnetic).

this period and the relatively rapid ozone recovery after the maximum intensity of the solar event.

[13] Ozone on six pressure levels at geographic latitudes 70°–82°S are indicated in Figure 5. This graph illustrates the ozone variation during the SPEs at 0.5, 1, 2, 4, 7, and 10 hPa from 26 October through 1 November. It is fairly clear that ozone has decreased at the highest two levels (0.5 and 1 hPa) from 28–30 October during the maximum intensity of the solar protons in 2003. The SPE-caused ozone changes at the lower four levels are less obvious since they are concealed by the sinusoidal ozone variations. These ozone fluctuations at 2, 4, 7, and 10 hPa are not caused by 24-hour oscillations; rather they are the result of measurements at different longitudes within the polar cap as a function of time.

4.2. NO_x ($NO + NO_2$)

[14] The Upper Atmosphere Research Satellite (UARS) Halogen Occultation Experiment (HALOE) measured NO and NO_2 during these SPEs at high southern latitudes. HALOE measured NO and NO_2 (NO_x) from 12–15 October over the 71°–74°S latitude range at sunrise before the SPEs. The average of these measurements is shown in Figure 6. Note that NO_x reaches a maximum of ~11 ppbv at about 3 hPa and then decreases rapidly to less than 1 ppbv by 0.3 hPa and stays at those reduced levels up to 0.01 hPa. NO_x then increases rapidly to levels over 20 ppbv by 0.004 hPa.

[15] HALOE next viewed these high southern latitudes (62°–75°S) in the period 30 October through 7 November, this time at sunset, during and after the solar event period. Since NO and NO_2 are tightly coupled and the quantity $NO + NO_2$ is highly conserved during a 24-hour period in the upper stratosphere and mesosphere, it is possible to compare sunrise NO_x measurements with sunset NO_x measurements and derive the perturbed atmospheric NO_x values for a short period (approximately a week). This was done in constructing Figure 7, which shows the excess NO_x beyond the baseline amounts in Figure 6. A seven-point "boxcar" running average is applied to these HALOE data in this figure.

[16] NO_x values greater than 100 ppbv were produced in the middle to upper mesosphere (0.03 to 0.006 hPa) for 30–31 October. Increases in NO_x greater than 20 ppbv were found in the lower mesosphere throughout the time period (30 October through 7 November). These are clearly huge increases above the baseline values less than 1 ppbv and illustrate the dramatic change in middle atmospheric NO_x due to these SPEs. We next employ our global model in

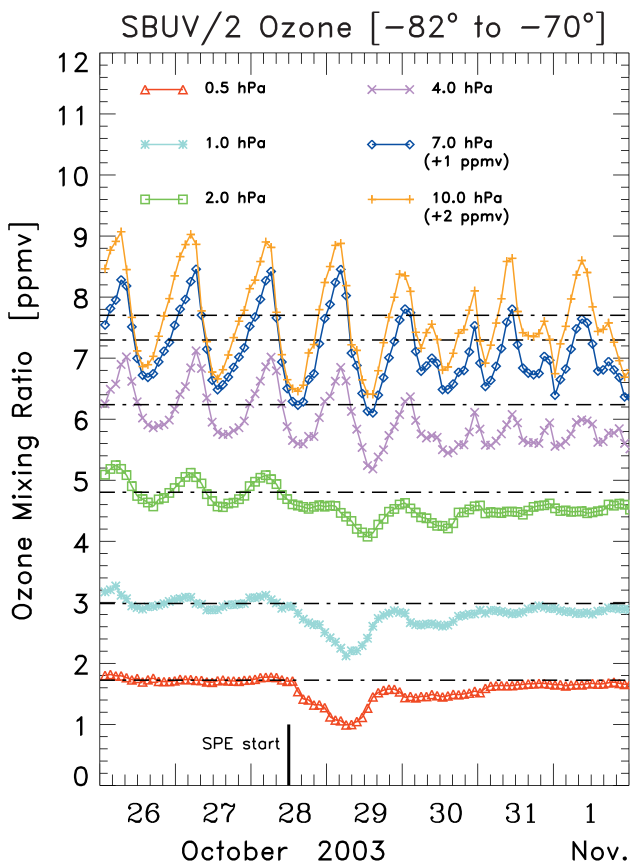

Figure 5. Polar Southern Hemisphere ozone observations from NOAA 16 SBUV/2 measurements for the 0.5, 1, 2, 4, 7, and 10 hPa levels during the 26 October through 1 November 2003 time period. The colored symbols with connected color lines indicate the measurements and the horizontal dashed-dotted lines indicate approximate average background observations. The symbols represent the average ozone abundance for each orbit at the specified pressure levels. Note that the 7 and 10 hPa data have been offset vertically for clarity.

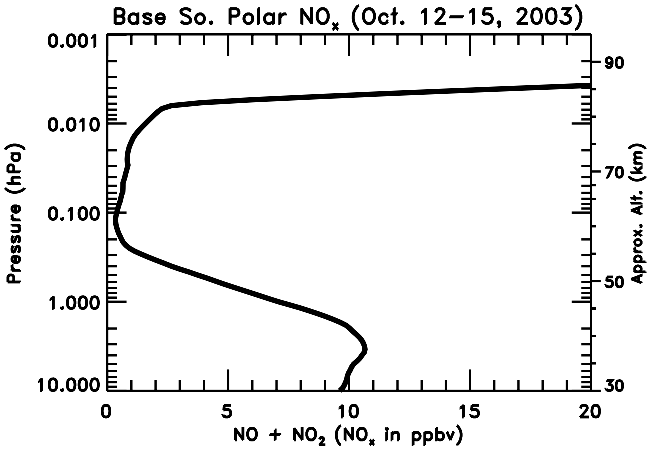

Figure 6. HALOE NO_x ($NO + NO_2$) average of sunrise measurements taken in the polar Southern Hemisphere (71°–74°S) from 12 to15 October 2003. Used as baseline to compute October–November 2003 SPEs influence.

simulations "with" and "without" the SPEs to aid in understanding these significant polar perturbations.

5. Model Predictions

5.1. Model Description

[17] The latest version of the Goddard Space Flight Center (GSFC) two-dimensional (2D) atmospheric model was used to predict the impact of solar protons on the atmosphere. This model was first discussed about 15 years ago [*Douglass et al.*, 1989; *Jackman et al.*, 1990] and has undergone extensive improvements over the years [e.g., *Considine et al.*, 1994; *Jackman et al.*, 1996; *Fleming et al.*, 1999]. The vertical range of the model, equally spaced in log pressure, is from the ground to approximately 90 km (0.0024 hPa) with approximately a 2 km grid spacing. Latitudes range from 85°S to 85°N with a 10° grid spacing.

[18] The transport is derived using the global winds and temperatures from the United Kingdom Meteorological Office (UKMO) data assimilation system for the years 1992–2000 and is described by *Fleming et al.* [2002]. For this paper we constructed a climatological average of the transport over these years and applied it over the simulated period from 2003 to 2005.

[19] The GSFC 2D chemistry solver has undergone significant upgrades in the past year. The ground boundary conditions for source gases N_2O, CH_4, CO_2, $CFCl_3$, CF_2Cl_2, $C_2Cl_3F_3$, $C_2Cl_2F_4$, C_2ClF_5, CCl_4, CH_3CCl_3, $CHClF_2$, $C_2H_3FCl_2$, $C_2H_3F_2Cl$, $C_2HF_3Cl_2$, $CBrClF_2$, $CBrF_3$, CBr_2F_2, and $C_2Br_2F_4$ are taken from *World Meteorological Organization (WMO)* [2003] for the particular simulated year. The ground boundary conditions for CO are assumed to be 150 ppbv in the Northern Hemisphere and 50 ppbv in the Southern Hemisphere. Water vapor (H_2O) is computed as described by *Fleming et al.* [1995] and HNO_3 is transported and computed separately from other NO_y species. A diurnal average computation is performed for these 19 source gases and HNO_3 without a diurnal cycle computation.

[20] The model computes seven chemical families, which include: (1) O_3; (2) $O(^3P)$, $O(^1D)$, and $O_2(^1\Delta)$; (3) H, OH, HO_2, and H_2O_2; (4) N, NO, NO_2, NO_3, N_2O_5, HO_2NO_2, and HONO; (5) Cl, ClO, HCl, HOCl, $ClONO_2$, ClO_3, OClO, Cl_2O_2, Cl_2, and $ClNO_2$; (6) Br, BrO, HBr, HOBr, $BrONO_2$, Br_2, and BrCl; and (7) CH_2O, CH_3O_2, and CH_3OOH. A diurnal cycle is computed for all thirty-five of these constituents within the seven families using the technique developed for the Atmospheric Environmental Research (AER) 2D model [*Weisenstein et al.*, 1991, 2004; *Rinsland et al.*, 2003]. The scheme allows for ten time steps in the day and five time steps in the night of a 24-hour period. The technique also provides a computation at sunrise and sunset, which allows easy comparisons with satellite solar occultation measurements. The seven families, 19 source gases and HNO_3 are all transported separately once each 24-hour period. The photochemical gas and heterogeneous reaction rates and photolysis cross sections are updated to the latest Jet Propulsion Laboratory recommendations [*Sander et al.*, 2003] for these computations.

5.2. Model Simulations

[21] The GSFC 2D model was used in two primary simulations, "base" and "perturbed," for the years 2003–2005. The base simulation includes no SPEs, whereas the perturbed simulation includes all SPEs in the period 26 October through 7 November 2003.

[22] The starting conditions for both the base and perturbed simulations were provided by a time dependent "spin-up" simulation from January 1980 through September 2003, which included the appropriate source gas boundary conditions from *WMO* [2003]. The base simulation continued this time dependent computation over the years October 2003 through December 2005.

[23] The perturbed simulation started from the end of the spin-up simulation and also included the HO_x and NO_y production by the October–November 2003 SPEs in the northern and southern polar regions. The HO_x produc-

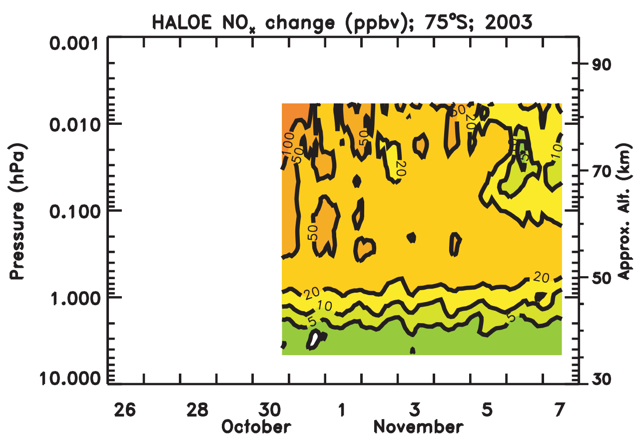

Figure 7. Polar Southern Hemisphere NO_x ($NO + NO_2$) change from ambient atmosphere amounts caused by October–November 2003 SPEs from HALOE sunset measurements taken 30 October through 7 November between 62° and 75°S subtracted from the baseline values given in Figure 6. Contour levels are 2, 5, 10, 20, 50, and 100 ppbv.

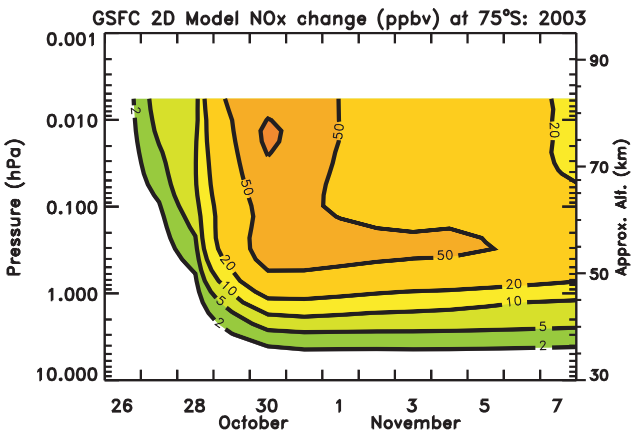

Figure 8. Polar Southern Hemisphere NO_x ($NO + NO_2$) change from ambient atmosphere amounts caused by October–November 2003 SPEs from GSFC 2D model results from 26 October through 7 November, which were computed by subtracting the base from the perturbed simulation. Contour levels are 2, 5, 10, 20, 50, and 100 ppbv.

tion by the SPEs was included by scaling the ion pair production rates given in Figure 2 with the values provided in *Solomon et al.* [1981, Figure 2], which showed the HO_x production as a function of altitude and ion pair production rate. Additional discussion of HO_x production by SPEs is given in section 3.1.

[24] The NO_y production by the SPEs was included by scaling the ion pair production rates given in Figure 2 assuming 0.55 $N(^4S)$ atoms per ion pair and 0.7 NO molecules per ion pair. More discussion of these NO_y scaling factors is included in section 3.2.

[25] Solar protons generally impact both hemispheres over the entire polar cap region (poleward of a cutoff geomagnetic latitude of about 60°) with relatively minor access outside this region. Although there is some deviation to this assumption for certain SPEs [*Blake et al.*, 2001; *Leske et al.*, 2001], the Oct.–Nov. 2003 SPEs generally followed this supposition (e.g., see Figure 4).

[26] For the purposes of this study, we assumed that the solar protons deposited their energy in both hemispheres at geomagnetic latitudes above 60°. Since our model is based on a geographic latitude coordinate and since the geomagnetic poles are offset by about 11° from the geographic poles, this results in weightings for particle influences of 1.0 for model grid boxes centered on ±85°, 0.98 for ±75°, 0.60 for ±65°, 0.31 for ±55°, 0.02 for ±45°, and 0.0 for all other latitudes.

5.3. Short-Term Computed Constituent Changes Due to SPEs

5.3.1. NO_x

[27] There are very significant atmospheric changes simulated during and shortly after the SPEs that occurred in Oct.–Nov. 2003. The modeled NO_x changes from SPEs are computed by subtracting the base from the perturbed simulation and are given in Figure 8. Enhancements in NO_x are computed as early as 26 October due to the increased proton fluxes evident on that day in Figure 1. The NO_x changes maximized above 100 ppbv on 30 October near 0.01–0.02 hPa, just after the huge enhanced proton fluxes during the peak of this solar active period. NO_x increases >50 ppbv in the lower mesosphere (0.2–0.4 hPa) continued through about Nov. 5.

[28] The modeled NO_x changes are fairly similar to the HALOE measurements. For example, both the model and measurements show (1) the largest NO_x enhancements above 0.1 hPa; (2) the NO_x endurance is longest below 0.1 hPa; and (3) the enhancements are quantitatively similar throughout most of the pressure domain and over most of the time period.

[29] There are some differences between the modeled NO_x changes and the HALOE measurements. For example, it does appear that the NO_x above 0.1 hPa is reduced more rapidly in the observations than simulated. This difference may be related to the fact that the model results are all taken at 75°S, whereas the measurements are a combination of measurements from 75°S (30 October) down to 62°S (7 November).

5.3.2. OH

[30] Among the largest computed atmospheric changes due to the Oct.–Nov. 2003 SPEs are those of OH. The OH computed changes are shown in Figure 9a in the Southern polar cap region. We show model computations for 85°S, deep within the polar cap to insure that the full impact of the solar protons is computed. Increases of OH greater than 100% were calculated for days 28–30 October and 3–4 November in the mesosphere. Enhancements of OH greater than 10% only extended to the stratosphere on 3 days, 28–30 October. These OH increases are largest during the SPEs and the OH enhancements persisted only for a few hours after the SPEs (see Figure 2). HO_x constituents are very reactive with each other and thus have a relatively short lifetime [e.g., *Solomon et al.*, 1981].

5.3.3. Ozone

[31] The produced HO_x constituents drive practically all the ozone depletion in the mesosphere and the upper stratosphere during the SPEs. Several HO_x catalytic destruction cycles are important in the mesosphere and stratosphere. For example, the catalytic cycle

$$H + O_3 \rightarrow OH + O_2 \quad (4)$$

$$OH + O \rightarrow H + O_2 \quad (5)$$

$$\text{Net} \qquad O_3 + O \rightarrow O_2 + O_2$$

is important in the middle and upper mesosphere and the catalytic cycle

$$OH + O_3 \rightarrow HO_2 + O_2 \quad (6)$$

$$HO_2 + O \rightarrow OH + O_2 \quad (7)$$

$$\text{Net} \qquad O_3 + O \rightarrow O_2 + O_2$$

is important in the lower mesosphere and upper stratosphere.

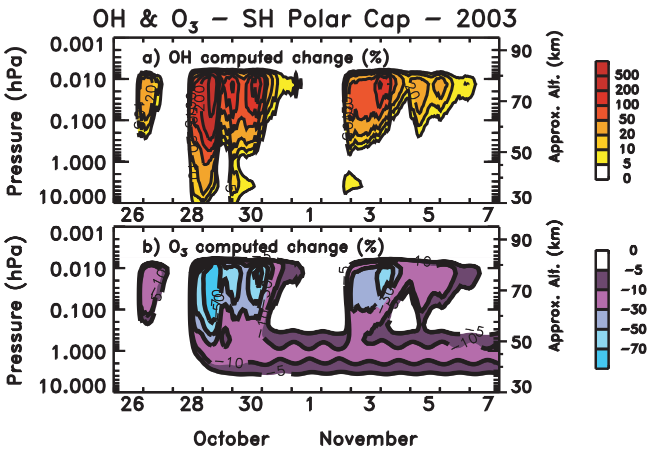

Figure 9. Southern Hemisphere polar cap (85°S) GSFC 2D model results from 26 October through 7 November, which were computed by comparing the perturbed to the base simulation for (a) OH percentage change with contour levels +5, +10, +20, +50, +100, +200, and +500% and (b) O_3 percentage change for contour levels −5, −10, −30, −50, and −70%.

[32] Substantial ozone decreases are computed in the mesosphere and shown in Figure 9b. Decreases greater than 70% are calculated on 29 October between 0.2 and 0.007 hPa. Short-lived ozone depletions >30% are calculated for the mesosphere in two periods, 28–31 October and 3–4 November, roughly corresponding to the altitude range and periods of enhanced OH levels >50%.

[33] More continuous computed ozone decreases (>5%) in the lower mesosphere and upper stratosphere are apparent over the 28 October through 7 November period. These longer-term ozone depletions are caused by the NO_x enhancements from the SPEs for that region of the atmosphere (see Figures 7 and 8). The slight oscillation in the computed ozone change values is caused by the 24-hour variation in solar zenith angle at 85°S. The SPE-caused ozone depletion has a fairly strong solar zenith angle dependence.

[34] It is not possible to compare our modeled ozone changes with the HALOE measurements. The base HALOE ozone measurements before the SPEs (see, also, section 4.2) were taken at sunrise in the southern polar region, whereas the perturbed measurements were taken at sunset in approximately the same geographic region. Since mesospheric ozone changes dramatically over a 24-hour period, a comparison of these sunrise and sunset measurements would lead to an inaccurate quantitative ozone change. We are, however, able to compare to NOAA-16 SBUV/2 ozone measurements (see Figure 5).

[35] In order to effectively compare our modeled ozone changes to these SBUV/2 measurements, we compute a "smoothed" 13-point running boxcar average of those data for the four pressure levels 2, 4, 7, and 10 hPa. The smoothing is applied to reduce the periodic oscillations discussed at the end of section 4.1 for easier interpretation of longer-term ozone changes. These SBUV/2 ozone data (smoothed for 2, 4, 7, and 10 hPa; and nonsmoothed for 0.5 and 1 hPa) are presented in Figure 10. Large ozone decreases are evident at the higher altitudes with 10, 30, and 40% maximum decreases on 29 October at 2, 1, and 0.5 hPa, respectively.

[36] Longer-term SBUV/2 ozone depletion between 5 and 8% are observed at levels 2, 4, and 7 hPa. The model calculated ozone depletions are given in Figure 10 and represented via the solid black line at each pressure level. The computed ozone at each pressure level is slightly different from the measured values, thus for ease of comparison the percentage modeled ozone deviations from the horizontal reference values (represented by the light dash-dot lines) are shown. These reference values are: 1.73 ppmv (0.5 hPa), 3.0 ppmv (1 hPa), 4.8 ppmv (2 hPa), 6.24 ppmv (4 hPa), 6.3 ppmv (7 hPa), and 5.7 ppmv (10 hPa).

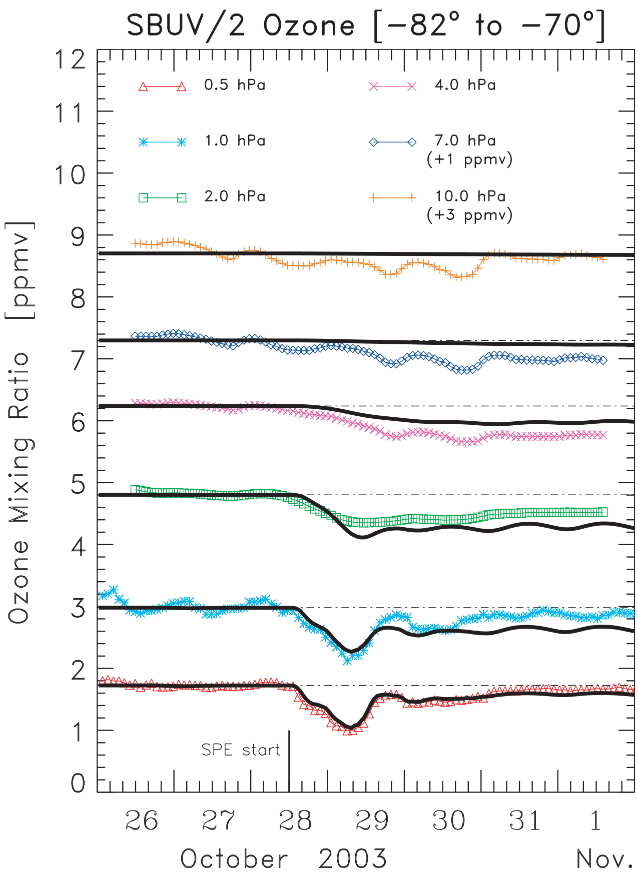

Figure 10. Polar Southern Hemisphere ozone observations from NOAA 16 SBUV/2 measurements for the 0.5, 1, 2, 4, 7, and 10 hPa levels during the 26 October through 1 November 2003 time period. As in Figure 5, the colored symbols with connected color lines indicate the measurements and the horizontal dashed-dotted lines indicate approximate average background observations. The SBUV/2 measurements for the lower four levels (2, 4, 7, and 10 hPa) were smoothed with a 13-point sliding boxcar average. GSFC 2D model results are represented by the solid black line. Note that the 7 and 10 hPa data have been offset vertically for clarity.

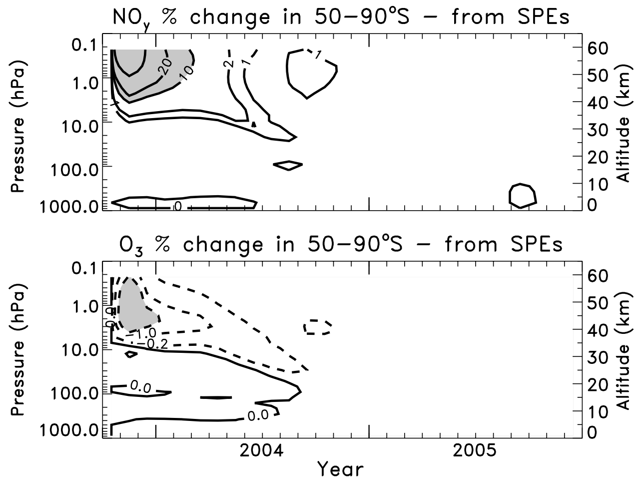

Figure 11. GSFC 2D model computed percentage changes in NO_y and O_3 for the polar Southern Hemisphere area (50°–90°S) in the time period October 2003 through December 2005 resulting from the October–November 2003 SPEs. Contour levels for NO_y (top plot) are 0, +1, +2, +10, +20, and +100%. The gray highlighted areas for NO_y indicate increases of greater than 10%. Contour levels for O_3 (bottom plot) are −2, −1, −0.2, 0, and +0.2%. The gray highlighted areas for O_3 indicate decreases greater than 2%. These changes were computed by comparing the perturbed to the base simulation.

[37] The modeled ozone change represents fairly well the SBUV/2 maximum decreases at the highest levels (0.5 and 1 hPa), however, at lower levels the model does less well. The model appears to predict a larger (smaller) ozone decrease as a result of the SPEs at 1 and 2 hPa (4 and 7 hPa) for the last three days of the plot (30 October through 1 November).

[38] The "apparent" measured ozone change at 10 hPa is noteworthy as no ozone decrease has been observed during a SPE at this low an altitude. Our model (solid black line) predicts no ozone change as a result of the Oct.–Nov. 2003 SPEs at this pressure level. Another stratospheric ozone phenomenon is also ongoing at this time of the year, the "Antarctic ozone hole." Further investigation into the apparent measured ozone changes has revealed that these decreases are caused by ozone depletions at pressures higher than 10 hPa being dynamically driven upward to cause a fluctuation in ozone at this higher altitude.

5.4. Long-Term Computed Constituent Changes Due to SPEs

5.4.1. NO_y

[39] The enhancements of NO and NO_2 from SPEs elevate the amount of other NO_y constituents over the course of a few days. The NO_y family can have a lifetime of months to years, if it is transported to the middle and lower stratosphere [e.g., *Jackman et al.*, 2000; *Randall et al.*, 2001]. The percentage change of NO_y in the Polar Regions, 50°–90°S and 50°–90°N, is computed for $2^1/_4$ years and shown in Figures 11 and 12. NO_y enhancements >10% persist for only about five months in the middle atmosphere in the Southern polar region. The sunlight is intense during this period in the Southern Hemisphere (SH) and odd nitrogen is rapidly lost via

$$NO + h\nu(< 191\ \mathrm{nm}) \rightarrow N + O \tag{8}$$

followed by

$$N + NO \rightarrow N_2 + O \tag{9}$$

The winds are also generally upward in the late spring/summer seasons, thus NO_y constituents are transported upward to the higher altitudes, where the loss process is greater.

[40] This two-step loss process represented by reactions (8) and (9) goes much slower in the Northern Hemisphere (NH) at this time of year (late fall/winter) due to the lower amount of sunlight. NO_y enhancements >10% endure for nearly 9 months in the middle atmosphere with the strongest persistence in the middle stratosphere. Computed NO_y enhancements >2% even persist for over 2 years past the SPEs in the low to middle stratosphere.

[41] In summary, although the production of NO_y constituents is the same in both hemispheres, the NO_y constituents have a much larger impact in the northern polar latitudes than the southern polar latitudes. This is caused by the seasonal differences between the two hemispheres at

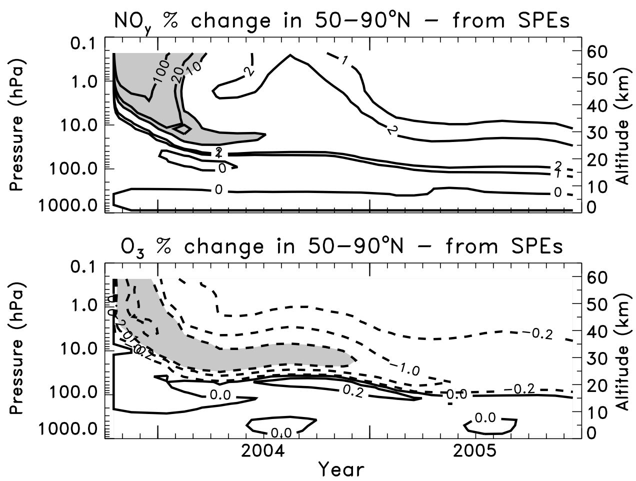

Figure 12. GSFC 2D model computed percentage changes in NO_y and O_3 for the polar Northern Hemisphere area (50°–90°N) in the time period October 2003 through December 2005 resulting from the October–November 2003 SPEs. Contour levels for NO_y (top plot) are 0, +1, +2, +10, +20, and +100%. The gray highlighted areas for NO_y indicate increases of greater than 10%. Contour levels for O_3 (bottom plot) are −10, −2, −1, −0.2, 0, and +0.2%. The gray highlighted areas for O_3 indicate decreases greater than 2%. These changes were computed by comparing the perturbed to the base simulation.

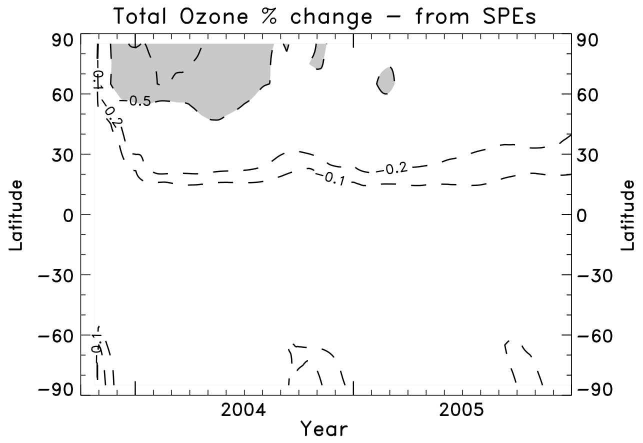

Figure 13. GSFC 2D model computed percentage total ozone changes for the time period October 2003 through December 2005 resulting from the October–November 2003 SPEs. Contour levels are −1, −0.5, −0.2, and −0.1%. The gray highlighted areas indicate total ozone decreases greater than 0.5%. These changes were computed by comparing the perturbed to the base simulation.

the time the event occurred, i.e., fall/winter in NH, spring/summer in SH (see Figures 11 and 12).

5.4.2. Ozone

5.4.2.1. Profile Ozone

[42] Associated ozone decreases follow the enhanced NO_y amounts. Ozone is reduced by the NO_x constituents through the following primary catalytic destruction cycle:

$$NO + O_3 \rightarrow NO_2 + O_2 \tag{10}$$

$$NO_2 + O \rightarrow NO + O_2 \tag{11}$$

$$\text{Net} \quad O_3 + O \rightarrow O_2 + O_2$$

This NO_y-caused catalytic destruction process acts on ozone over a period of time leading to ozone loss at lower altitudes (middle to lower stratosphere), essentially wherever NO_y is transported (see Figures 11 and 12). More ozone loss is predicted in the northern polar region simply because more NO_y survives in this hemisphere. Ozone decreases >2% persist for 13 months past the SPEs in the middle stratosphere.

[43] SPE-produced ozone increases are computed for years 2004–2005 below about 30 hPa. These increases are caused by the interference of the long-lived SPE-produced NO_y with the chlorine and bromine loss cycles for ozone destruction. This characteristic has been noticed before in other studies of very large SPEs [e.g., *Jackman et al.*, 2000].

5.4.2.2. Total Ozone

[44] The impact of the Oct.–Nov. 2003 SPEs on total ozone is shown in Figure 13. Total ozone is reduced by a maximum of about 1% for about three months in the winter/early spring of the Northern polar region. These maximum total ozone changes are not predicted to occur during the SPEs; rather the transport of the enhanced NO_y to lower altitudes (and higher ambient ozone amounts) allows more substantial total ozone impact. Total ozone reductions >0.5% are predicted to persist for over 8 months in the Northern polar latitudes. Total ozone depletions in the Southern Hemisphere are predicted to be much less with levels never exceeding 0.5%.

6. Conclusions

[45] The impact of the large solar storms in October–November 2003 with their accompanying solar protons on the Earth's middle atmospheric polar cap regions was measured and modeled. There were several periods of intense proton fluxes entering the atmosphere with the most intense occurring 28–31 October 2003, the fourth largest period of SPEs in the past 40 years. HO_x constituents were predicted to increase substantially over the 26 October through 7 November period with computed enhancements of >100% in mesospheric OH for a few days. NO_y constituents were measured and predicted to increase as well. The NO_x ($NO + NO_2$) amount was observed to increase by over 20 ppbv throughout the Southern polar mesosphere with the UARS HALOE instrument; similar increases were computed by the GSFC 2D model.

[46] The computed HO_x enhancements caused middle to upper mesospheric ozone depletions of >70% during the most intense period of solar protons (29 October). The NOAA 16 SBUV/2 instrument measured a short-term ozone depletion of 40% and 30% at 0.5 hPa (lower mesosphere) and 1 hPa (upper stratosphere), respectively, and were probably a result of the HO_x increases. SBUV/2 observations showed ozone depletions of 5–8% in the polar upper stratosphere lasting days beyond the events, most likely a result of the NO_y enhancements. Longer-term Northern Hemisphere polar total ozone decreases of >0.5% were predicted to last for over eight months past the events with the GSFC 2D model. Clearly, the October–November 2003 SPEs were responsible for a substantial perturbation to the polar neutral middle atmosphere.

[47] **Acknowledgments.** We thank NASA Headquarters Atmospheric Chemistry Modeling and Analysis Program for support during the time that this manuscript was written. We also thank the NOAA GOES team for providing the solar proton flux data over the Internet. The SBUV/2 data were obtained from NOAA/NESDIS with support from the NOAA Climate and Global Change Atmospheric Chemistry Element. We thank two anonymous reviewers for valuable comments and criticisms that led to an improved manuscript.

[48] Arthur Richmond thanks Alexander Zadorozhny and another reviewer for their assistance in evaluating this paper.

References

Blake, J. B., M. C. McNab, and J. E. Mazur (2001), Solar proton cap intensity structures as a test of magnetic field models, *Adv. Space Res.*, *28*(12), 1753–1757.

Considine, D. B., A. R. Douglass, and C. H. Jackman (1994), Effects of a polar stratospheric cloud parameterization on ozone depletion due to stratospheric aircraft in a two-dimensional model, *J. Geophys. Res.*, *99*, 18,879–18,894.

Crutzen, P. J., I. S. A. Isaksen, and G. C. Reid (1975), Solar proton events: Stratospheric sources of nitric oxide, *Science*, *189*, 457–458.

Douglass, A. R., C. H. Jackman, and R. S. Stolarski (1989), Comparison of model results transporting the odd nitrogen family with results transporting separate odd nitrogen species, *J. Geophys. Res.*, *94*, 9862–9872.

Fleming, E. L., S. Chandra, C. H. Jackman, D. B. Considine, and A. R. Douglass (1995), The middle atmospheric response to short and long term solar UV variations: Analysis of observations and 2D model results, *J. Atmos. Terr. Phys.*, *57*, 333–365.

Fleming, E. L., C. H. Jackman, R. S. Stolarski, and D. B. Considine (1999), Simulation of stratospheric tracers using an improved empirically based two-dimensional model transport formulation, *J. Geophys. Res.*, *104*, 23,911–23,934.

Fleming, E. L., C. H. Jackman, J. E. Rosenfield, and D. B. Considine (2002), Two-dimensional model simulations of the QBO in ozone and tracers in the tropical stratosphere, *J. Geophys. Res.*, *107*(D23), 4665, doi:10.1029/2001JD001146.

Frederick, J. E. (1976), Solar corpuscular emission and neutral chemistry in the Earth's middle atmosphere, *J. Geophys. Res.*, *81*, 3179–3186.

Heath, D. F., A. J. Krueger, and P. J. Crutzen (1977), Solar proton event: Influence on stratospheric ozone, *Science*, *197*, 886–889.

Hilsenrath, E., R. P. Cebula, M. T. DeLand, K. Laamann, S. Taylor, C. Wellemeyer, and P. K. Bhartia (1995), Calibration of the NOAA 11 solar backscatter ultraviolet (SBUV/2) ozone data set from 1989 to 1993 using in-flight calibration data and SSBUV, *J. Geophys. Res.*, *100*, 1351–1366.

Jackman, C. H., and R. D. McPeters (2004), The effect of solar proton events on ozone and other constituents, in *Solar Variability and Its Effects on Climate*, *Geophys. Monogr. Ser.*, vol. 141, edited by J. M. Pap and P. Fox, pp. 305–319, AGU, Washington, D. C.

Jackman, C. H., J. E. Frederick, and R. S. Stolarski (1980), Production of odd nitrogen in the stratosphere and mesosphere: An intercomparison of source strengths, *J. Geophys. Res.*, *85*, 7495–7505.

Jackman, C. H., A. R. Douglass, R. B. Rood, R. D. McPeters, and P. E. Meade (1990), Effect of solar proton events on the middle atmosphere during the past two solar cycles as computed using a two-dimensional model, *J. Geophys. Res.*, *95*, 7417–7428.

Jackman, C. H., E. L. Fleming, S. Chandra, D. B. Considine, and J. E. Rosenfield (1996), Past, present, and future modeled ozone trends with comparisons to observed trends, *J. Geophys. Res.*, *101*, 28,753–28,767.

Jackman, C. H., E. L. Fleming, and F. M. Vitt (2000), Influence of extremely large solar proton events in a changing stratosphere, *J. Geophys. Res.*, *105*, 11,659–11,670.

Jackman, C. H., R. D. McPeters, G. J. Labow, E. L. Fleming, C. J. Praderas, and J. M. Russell (2001), Northern hemisphere atmospheric effects due to the July 2000 solar proton event, *Geophys. Res. Lett.*, *28*, 2883–2886.

Krivolutsky, A., A. Kuminov, T. Vyushkova, N. Pereyaslova, and M. Nazarova (2003), Proton activity of the Sun during 23rd solar maximum and its response in ozonosphere of the Earth, *Adv. Space Res.*, *31*(9), 2151–2156.

Leske, R. A., et al. (2001), Observations of geomagnetic cutoff variations during solar energetic particle events and implications for the radiation environment at the Space Station, *J. Geophys. Res.*, *106*, 30,011–30,022.

McPeters, R. D. (1986), A nitric oxide increase observed following the July 1982 solar proton event, *Geophys. Res. Lett.*, *13*, 667–670.

Porter, H. S., C. H. Jackman, and A. E. S. Green (1976), Efficiencies for production of atomic nitrogen and oxygen by relativistic proton impact in air, *J. Chem. Phys.*, *65*, 154–167.

Randall, C. E., D. E. Siskind, and R. M. Bevilacqua (2001), Stratospheric NO_x enhancements in the southern hemisphere polar vortex in winter and spring of 2000, *Geophys. Res. Lett*, *28*, 2385–2388.

Rees, M. H. (1989), *Physics and Chemistry of the Upper Atmosphere*, pp. 278–281, Cambridge Univ. Press, New York.

Rinsland, C. P., D. K. Weisenstein, M. K. W. Ko, C. J. Scott, L. S. Chiou, E. Mahieu, R. Zander, and P. Demoulin (2003), Post-Mount Pinatubo eruption ground-based infrared stratospheric column measurements of HNO_3, NO, and NO_2 and their comparison with model calculations, *J. Geophys. Res.*, *108*(D15), 4437, doi:10.1029/2002JD002965.

Rusch, D. W., J.-C. Gerard, S. Solomon, P. J. Crutzen, and G. C. Reid (1981), The effect of particle precipitation events on the neutral and ion chemistry of the middle atmosphere, 1. Odd nitrogen, *Planet. Space Sci*, *29*, 767–774.

Sander, S. P., et al. (2003), Chemical kinetics and photochemical data for use in atmospheric studies, *JPL Publ. 02–25*.

Seppälä, A., P. T. Verronen, E. Kyrölä, S. Hassinen, L. Backman, A. Hauchecorne, J. L. Bertaux, and D. Fussen (2004), Solar proton events of October–November 2003: Ozone depletion in the Northern Hemisphere polar winter as seen by GOMOS/Envisat, *Geophys. Res. Lett.*, *31*, L19107, doi:10.1029/2004GL021042.

Solomon, S., D. W. Rusch, J.-C. Gerard, G. C. Reid, and P. J. Crutzen (1981), The effect of particle precipitation events on the neutral and ion chemistry of the middle atmosphere, 2, Odd hydrogen, *Planet. Space Sci.*, *29*, 885–892.

Solomon, S., G. C. Reid, D. W. Rusch, and R. J. Thomas (1983), Mesospheric ozone depletion during the solar proton event of July 13, 1982, 2, Comparison between theory and measurements, *Geophys. Res. Lett.*, *10*, 257–260.

Stolarski, R. S., G. J. Labow, and R. D. McPeters (1997), Springtime Antarctic total ozone measurements in the early 1970's from the BUV instrument on Nimbus 4, *Geophys. Res. Lett.*, *24*, 591–594.

Swider, W., and T. J. Keneshea (1973), Decrease of ozone and atomic oxygen in the lower mesosphere during a PCA event, *Planet. Space Sci.*, *21*, 1969–1973.

Vitt, F. M., and C. H. Jackman (1996), A comparison of sources of odd nitrogen production from 1974 through 1993 in the Earth's middle atmosphere as calculated using a two-dimensional model, *J. Geophys. Res.*, *101*, 6729–6739.

Weeks, L. H., R. S. CuiKay, and J. R. Corbin (1972), Ozone measurements in the mesosphere during the solar proton event of 2 November 1969, *J. Atmos. Sci.*, *29*, 1138–1142.

Weisenstein, D. K., M. K. W. Ko, J. M. Rodriguez, and N.-D. Sze (1991), Impact of heterogeneous chemistry on model-calculated ozone change due to High Speed Civil Transport aircraft, *Geophys. Res. Lett.*, *18*, 1991–1994.

Weisenstein, D. K., et al. (2004), Separating chemistry and transport effects in 2–D models, *J. Geophys. Res.*, *109*, D18310, doi:10.1029/2004JD004744.

World Meteorological Organization (WMO) (2003), Scientific Assessment of Ozone Depletion: 2002, *Rep. 47*, Global Ozone Res. and Monit. Proj., Geneva.

Zadorozhny, A. M., G. A. Tuchkov, V. N. Kikhtenko, J. Lastovicka, J. Boska, and A. Novak (1992), Nitric oxide and lower ionosphere quantities during solar particle events of October 1989 after rocket and ground-based measurements, *J. Atmos. Terr. Phys.*, *54*, 183–192.

M. T. DeLand, Science Systems and Applications, Inc., 10210 Greenbelt Road, Suite 400, Lanham, MD 20706, USA. (matthew_deland@ssaihq.com)

E. L. Fleming, C. H. Jackman, and G. J. Labow, Code 916, NASA Goddard Space Flight Center, Greenbelt Road, Greenbelt, MD 20771-0001, USA. (fleming@kahuna.gsfc.nasa.gov; charles.h.jackman@nasa.gov; labow@qhearts.gsfc.nasa.gov)

M. K. W. Ko, Mail Stop 401B, NASA Langley Research Center, Hampton, VA 23681, USA. (malcolm.k.ko@nasa.gov)

J. M. Russell, Center for Atmospheric Sciences, Hampton University, Hampton, VA 23668, USA. (james.russell@hamptonu.edu)

M. Sinnhuber, Institute of Environmental Physics, University of Bremen, Germany. (miriam@iup.physik.uni-bremen.de)

D. K. Weisenstein, Atmospheric and Environmental Research, Inc., 131 Hartwell Avenue, Lexington, MA 02421, USA. (weisenstein@aer.com)